MASTER THESIS

Thesis submitted in fulfillment of the requirements for the degree of Master of Science in Engineering at the University of Applied Sciences Technikum Wien - Degree Program Robotics Engineering

Alogrithmic Payload Estimation

By: Moritz Dönges, BSc

Student Number: 2310331024

Supervisor: Michael Schebeck, MSc

Vienna, November 27, 2025

Declaration

Vienna, November 27, 2025   Signature

Kurzfassung

Im Kontext der digitalen Fabrik an der UAS Technikum Wien, wo Menschen und Roboter sich die Aufgaben und den Arbeitsbereich teilen, ist die sichere und effiziente Handhabung von Nutzlasten von entscheidender Bedeutung. In der digitalen Fabrik der UAS werden Nutzlasten derzeit noch ohne Kenntnis ihrer internen Parameter gehandhabt, was zu potenziellen Manipulationsfehlern führen kann, die Menschen Schaden zufügen. Diese Studie beschreibt die Entwicklung einer fortschrittlichen Methode zur Kraft-/Drehmomentabschätzung, um die Fähigkeit eines UR5-Roboters zu verbessern, verschiedene Nutzlastbedingungen zu erkennen und zu handhaben. Diese Fähigkeit gewährleistet die Wahrnehmung des auf einer mobilen Industrieroboterplattform montierten UR5-Roboters, um den sicheren und effizienten Transfer von Nutzlasten zwischen verschiedenen Arbeitsbereichen innerhalb der Fabrik zu erleichtern. Die modernsten Methoden zur Kraft-/Drehmomentabschätzung für Industrieroboter nutzen neuronale Netze und Gauß-Prozesse als führende Methoden für genaue Nutzlastabschätzungen. Es wurde ein Gauß-Prozess-Modell entwickelt, um die Kräfte und Drehmomente abzuschätzen, die vom Roboter bei der Ausführung von Trajektorien erzeugt werden. In einem zukünftigen Projekt kann das Bewusstsein für Nutzlasten auf dem UR5-Roboter hinzugefügt werden. Auf diese Weise zielt die Studie darauf ab, die Intelligenz von Robotersystemen in industriellen Umgebungen zu verbessern und den Weg für eine höhere Produktivität und Sicherheit in digitalen Fertigungsumgebungen zu ebnen. Dieses Projekt führte auch zu einer Simulation, die eine Grundlage für die Aufzeichnung der Sensordaten aus dem UR5-Interieur.

Schlagworte: Gaussian Process, Force Estimation, Newton/Euler, UR5 Robot, Rigid Body

Abstract

In the context of the digital factory, at UAS Technikum Vienna, where humans and robots share the tasks and the workspace, the safe and efficient handling of payloads is essential. At the UAS digital factory payload is still handled without recognising anything about the payloads internal parameters, leading to potential manipulation failures causing human harm. This study describes the development of an advanced force/torque estimation method to improve a UR5 robots ability to recognize and handle different payload conditions. This capability ensures the perception of the UR5 robot mounted on a mobile industrial robot platform to facilitate the safe and efficient transfer of payloads between different workspaces within the factory. The state of the art methods of force/torque estimation for industrial robots serve neuronal networks and gaussian processes as the leading methods for accurate payload estimations. A gaussian process model has been developed to estimate the forces and torques generated by the robot when executing trajectories. In a future project face, an awareness of payloads can be added on the UR5 robot. In this way, the study aims to improve the intelligence of robotic systems in industrial environments and pave the way for higher productivity and safety in digital manufacturing environments. This project face also yeelted in a simulation that provides a basis to record the sensor data from the UR5's internal sensors and a force/torque sensor and a pipeline to train and evaluate gaussian process models.

Acknowledgements

Hello, here is some text without a meaning. This text should show what a printed text will look like at this place. If you read this text, you will get no information. Really? Is there no information? Is there a difference between this text and some nonsense like "Huardest gefburn"? Kjift – not at all! A blind text like this gives you information about the selected font, how the letters are written and an impression of the look. This text should contain all letters of the alphabet and it should be written in of the original language. There is no need for special content, but the length of words should match the language.

Contents

1 Introduction

This chapter provides the common thread of the work and positions it within the broader field of robotic manipulation and human-robot collaboration. We first develop the motivation for the study, followed by a precise problem description, a formal problem statement, and the resulting aim of the work. Subsequent chapters present the State of the Art, the proposed methods, the experimental evaluation, a discussion of the results and their implications, and an outlook on future research directions.

1.1 Motivation

The motivation for this work is given in two subsections, where the Context subsection outlines the growing role of industrial and collaborative manipulators, while the Use Case subsection specifies a concrete manipulation scenario that requires accurate online identification of robot and payload parameters.

1.1.1 Context

As the robotics industry grows year over year, so does the number of robots operating around the world. It is estimated that there were approximately 3.4 million industrial robots in use worldwide in 2023 [1]. At the same time, the number of newly installed industrial robots has been increasing steadily since 2014; between 2021 and 2024, around 541 000 new industrial robots were installed per year [2]. Within this landscape, collaborative robots (cobots) represent about 10.5% of the industrial robot market, with 57 040 new units deployed in 2023, and annual cobot installations since 2020, 2022, and 2023 reaching roughly 50 000 units per year; importantly, these cobots are expected to complement rather than replace traditional industrial robots [3].
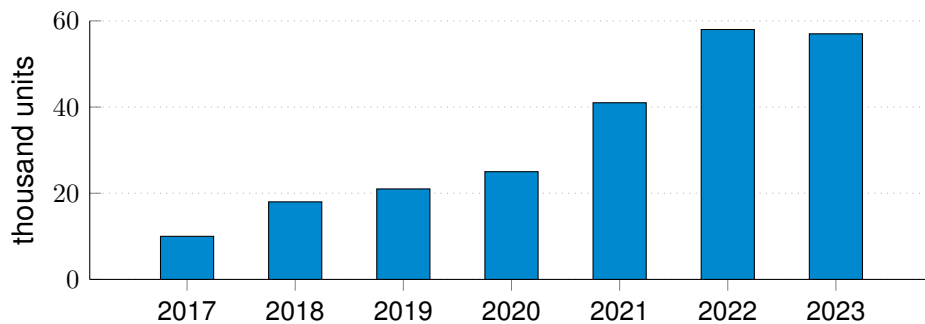

Figure 1: Global annual installations of collaborative robots from 2017 to 2023 (in thousand units). Data from [3].

The growing deployment of, and increasing collaboration with, robots imposes stringent requirements on safety and performance. As tasks become more complex and humans and robots share workspaces more closely, two closely related problems become central: safe manipulation of payloads and safe physical human-robot interaction. Addressing both problems requires accurate knowledge of the inertial parameters of the manipulated object together with consistent estimation of the robot's dynamic state and interaction forces. A collaborative robot must therefore maintain an internal representation of the mass-inertia properties of the payload or tool it manipulates and of the forces exchanged with its environment. This dynamic awareness is a prerequisite for compliant, contact-rich behaviour and for precise, high-performance manipulation in close proximity to humans. [4–15].

1.1.2 Use Case

The considerations above motivate a concrete use case in which a collaborative robotic arm must manipulate previously unseen objects in a shared workspace. A vision system can provide geometric information such as shape and dimensions of the payload, but it does not directly reveal its mass, center of mass (CoM), or inertia tensor. For safe and precise execution of contact-rich tasks, however, these inertial properties are indispensable.

In practice, the only viable way to obtain this information during operation is to exploit the robot's own sensor data, such as joint positions, velocities and accelerations, motor currents/torques, and optionally wrist force/torque measurements. From these signals, one can estimate both the robot's rigid-body parameters and the inertial properties of the attached payload. This leads to the dual identification problem of robot dynamic parameter identification (RDPI) and payload dynamic parameter identification (PDPI).

The targeted application scenario comprises typical industrial and collaborative tasks such as pick-and-place, human-assisted manipulation, and precise tool use. In all these cases, RDPI and PDPI must be performed online so that the controller maintains an up-to-date model of the combined robot-payload dynamics and the resulting contact forces. Robust online identification methods are therefore a key enabling technology for safe human-robot collaboration and high-performance manipulation with arbitrary payloads and tools.

Next is: use case, problem description (mathematical background), problem statement, contribution. Then state of the art.

1.2 Problem Statement

The subsection Mathematical Challenges in Dynamic Awareness analyses why endowing a robotic manipulator with awareness of its own dynamics, payload, and tools is mathematically demanding and cannot be achieved by simple calculation or direct measurement alone. The subsection Limitations of the Current State of the Art then identifies the main shortcomings of existing identification and estimation methods in the literature, thereby motivating the contribution of this work.

1.2.1 Kinematic and Dynamic Background of Robot Manipulation and Environment Interaction

The inertial properties of a rigid body are collected in the standard 10-dimensional parameter vector

$$\phi^T = \begin{bmatrix} m & mc_x & mc_y & mc_z & J_{xx} & J_{xy} & J_{xz} & J_{yy} & J_{yz} & J_{zz} \end{bmatrix} \in \mathbb{R}^{10}, \tag{1}$$

which enters the Newton–Euler equations

$$\begin{bmatrix} \mathbf{f} \\ \boldsymbol{\tau} \end{bmatrix} = m \begin{bmatrix} \mathbf{I}_{3\times3} & -[\mathbf{c}]^\times \\ [\mathbf{c}]^\times & \mathbf{J}_s \end{bmatrix} \begin{bmatrix} \mathbf{a} \\ \boldsymbol{\alpha} \end{bmatrix} + \begin{bmatrix} m[\boldsymbol{\omega}]^\times[\boldsymbol{\omega}]^\times \mathbf{c} \\ [\boldsymbol{\omega}]^\times \mathbf{J}_s \boldsymbol{\omega} \end{bmatrix}, \tag{2}$$

so that the wrench $(\mathbf{f}, \boldsymbol{\tau})$ depends nonlinearly on the motion $(\mathbf{a}, \boldsymbol{\alpha}, \boldsymbol{\omega})$ but linearly on ϕ.

For the equipment rigidly attached to the tool flange (gripper/tool, with or without pay-load/load) we define an effective rigid-body parameter vector

$$\phi_{\text{eff}} = \begin{cases} \phi_{\text{tool}}, & \text{no load,} \\[2mm] \phi_{\text{tool}} + \phi_{\text{load}}, & \text{with load,} \end{cases} \tag{3}$$

which acts on top of the nominal robot dynamics. In contrast, with a clean flange (no tool/no load) only the robot parameters ϕ_{robot} contribute to the system dynamics.

The robot structure itself is described by its own parameter vector ϕ_{robot}, which enters the standard joint-space rigid-body dynamics. We denote this contribution by $\boldsymbol{\tau}_{\text{robot}}$ (clean flange),

$$\boldsymbol{\tau}_{\text{robot}} = \mathbf{M}(\mathbf{q})\ddot{\mathbf{q}} + \mathbf{C}(\mathbf{q}, \dot{\mathbf{q}})\dot{\mathbf{q}} + \mathbf{G}(\mathbf{q}) + \boldsymbol{\tau}_f(\dot{\mathbf{q}}), \tag{4}$$

where $\boldsymbol{\tau}_f(\dot{\mathbf{q}})$ models joint-level non-idealities such as Coulomb and viscous friction, possible Stribeck effects, and drive-train phenomena like backlash.

The wrench generated by the effective rigid body at the flange induces an additional joint-space torque

$$\boldsymbol{\tau}_{\text{ext}} = \mathbf{J}^T(\mathbf{q})\, \vec{F}_{\text{ext}}(\phi_{\text{eff}}), \tag{5}$$

where $\mathbf{J}(\mathbf{q})$ is the end-effector Jacobian. In the clean-flange case (no tool/no load), $\vec{F}_{\text{ext}}$ reduces to purely external interaction forces with the environment (e.g. contacts or collisions).

The motor torques are therefore

$$\boldsymbol{\tau}_{\text{motor}} = \boldsymbol{\tau}_{\text{robot}} + \boldsymbol{\tau}_{\text{ext}}(\phi_{\text{eff}}), \tag{6}$$

and for brushless DC actuators with torque constant k_t one obtains the current–torque relation

$$\boldsymbol{\tau}_{\text{motor}} = k_t\, \boldsymbol{I} \quad \Rightarrow \quad \boldsymbol{I} = \frac{\boldsymbol{\tau}_{\text{robot}} + \boldsymbol{\tau}_{\text{ext}}(\phi_{\text{eff}})}{k_t}. \tag{7}$$

If a force/torque sensor is mounted at the flange, the measured wrench can be written, using the relations derived in the Appendix, as

$$\vec{F}_{\text{measured}} = Y(\mathbf{a}, \boldsymbol{\alpha}, \boldsymbol{\omega})\, \phi_{\text{eff}} + \vec{F}_{\text{bias}} + \vec{n}, \tag{8}$$

where $Y(\cdot)$ is the 6×10 Newton–Euler regressor matrix defined in the Appendix. It is linear in the inertial parameter vector ϕ_{eff}, but depends nonlinearly on the motion variables $(\mathbf{a}, \boldsymbol{\alpha}, \boldsymbol{\omega})$. The terms $\vec{F}_{\mathrm{bias}}$ and $\vec{n}$ denote sensor bias and noise, respectively.[1] The motion variables $(\mathbf{a}, \boldsymbol{\alpha}, \boldsymbol{\omega})$ are in turn determined by the joint state and motor torques through the nonlinear dynamics (4)–(7).

From an identification viewpoint, this creates two tightly coupled challenges. First, all available measurements (joint currents, positions, velocities and flange wrench) depend on the combined dynamics of robot, tool and load via the nonlinear relationships (4)–(8), so the contribution of the load parameters ϕ_{load} cannot be isolated by simple computation or direct measurement. Second, accurate payload or load dynamic parameter identification (PDPI) presupposes an equally accurate compensation of the underlying robot–tool dynamics, including unmodelled effects such as friction and joint transmission nonlinearities. Together, these aspects make dynamic awareness of payload, tool and robot a mathematically demanding inverse problem rather than a straightforward calculation from geometric or sensor data.

1.2.2 Limitations of the Current State of the Art

1.3 Aim of Work

2 State of the Art

2.1 Research Strategy

- $C_1 =$ Classical / Observers

- $C_2 =$ Gaussian Process (GP)

- $C_3 =$ Deep Sequence Models (MLP / GRU / TCN / Transformer / LSTM)

- $C_4 =$ Physics-Informed / Differentiable

- $C_5 =$ Surveys

- $C_T =$ Goal & Domain Terms

  - $C_{mt} =$ Estimation & Modeling Terms

  - $C_{ct} =$ Robotics Context Terms

---

[1] All experiments in this work are simulation-based; in the subsequent method formulation, sensor bias and noise are therefore neglected and (8) is used without $\vec{F}_{\mathrm{bias}}$ and $\vec{n}$.
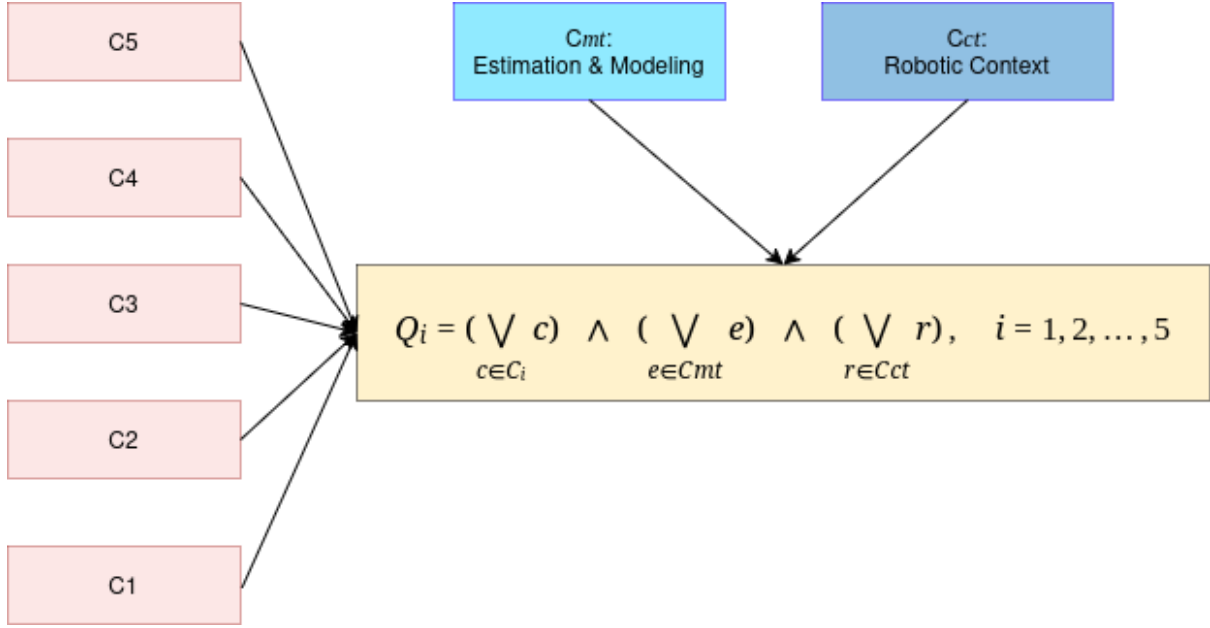
Figure 2: Query logic used to categorise the SoA papers. Each category Q_i is formed by combining content clusters C_i with estimation & modelling terms C_{mt} and robotics context terms C_{ct}. The combined representation C and query set Q are formed by the union of their respective subsets.

Here is written that the terms of the categories are found in the appendix and why and how this Strategy is executed. Which then leads into the remaining 36 relevant SoA papers in this study.

Table 1: Overview of query results by category.

Query	Relev. SoA	Rigid-body	Payload	Both
$\mathbf{Q_1}$ = Classical / Observers	17	7	7	3
$\mathbf{Q_2}$ = Gaussian Process (GP)	4	4	0	0
$\mathbf{Q_3}$ = Deep Sequence Models	8	4	4	0
$\mathbf{Q_4}$ = Physics-Informed / Diff.	5	5	0	0
$\mathbf{Q_5}$ = Surveys	2	–	–	–
Total	**36**	**20**	**11**	**3**

2.2 One-page condensed SoA summary for Q1

Category Q1 groups classical **model-based methods for robot and payload dynamics and interaction force estimation**, mostly based on **linearly parameterised rigid-body dynamics (RBD) and LS/WLS regressors**, sometimes combined with observers and Kalman filters. Across the papers[8][9][10], **Least Squares (LS), Weighted LS (WLS) and LS-Newton-Euler (LS-NE) regressors** are the dominant tools for both **robot dynamic parameter identification**

(RDPI) and **payload dynamic parameter identification (PDPI)**. They are used in joint space, in motor-current space and in sensor frames, and provide **strong performance for mass, centre of mass (CoM) and joint-torque prediction** when trajectories are sufficiently exciting.

A large subset of works demonstrates that **neither a nominal CAD-based RBD model nor an FT sensor is strictly necessary**.[4],[16],[7],[17],[8], Q1.5–Q1.8, Q1.13, Q1.15 and Q1.16 build the regressor directly from measured joint states and controller torques, sometimes in **fully decoupled formulations** or via **residual-torque decomposition**. They use **constant-velocity/acceleration S-curve trajectories, Fourier trajectories or repeated sections** to decorrelate parameters and improve conditioning. These approaches typically obtain **very good mass estimates and acceptable CoM**, with **inertia remaining the weakest part of the identification**, especially for short trajectories.

Several methods employ **two-stage pipelines**: static poses for mass and CoM, followed by dynamic trajectories for inertia (e.g. Q1.5 and Q1.7). Q1.7 also shows that such schemes scale to **heavy ($\sim 40\,\mathrm{kg}$) payloads**, and can feed into **contact force estimation and compensation** with moderate batch times ($\approx 10\,\mathrm{s}$ for contact, $\approx 40\,\mathrm{s}$ for payload).

Where an **NRB model is available or identified offline**, it is commonly combined with **observers** for external torque and force estimation. Q1.2 and Q1.3 use LS-NE-based torque prediction together with **momentum or sliding-mode observers** to estimate external joint torques and EE forces. Q1.4 and Q1.17 combine RBD with **(adaptive) Kalman filters / disturbance observers** and explicit friction models (Stribeck or NN-based). These approaches can yield **good EE force estimation and collision detection**, but they are sensitive to model mismatch and friction modelling; Q1.17 reports good behaviour without external forces but large errors (up to $\approx 9\,\mathrm{Nm}$) under contact. **Sensorless interaction-force estimation** is addressed in Q1.3, Q1.12 and Q1.17. Q1.12, for example, uses LS-NE identification of $M(q)$, $C(q)$ and $G(q)$, then runs a **High-Order Finite-Time Observer (HOFFTO)** in joint space, using an FT sensor only as ground truth. This yields **good joint-torque prediction and acceptable EE force estimates**, but still depends on accurate offline dynamics. Finally, Q1.14 shows that combining LS-NE predicted torques with measured joint torques enables **robust collision detection and localisation of the collided joint** using simple residual thresholds, again assuming a reasonably accurate NRB model.

In summary, **Q1 methods show that classical LS-type identification and observers are mature and effective**:

- **Mass and CoM** can be identified very reliably, even **without NRB and without FT sensors**.

- **Inertia** is consistently harder and requires **carefully designed dynamic excitation**, and still tends to be less accurate or weakly validated.

- **Torque prediction, contact detection and simple EE force estimation** are already at a high level with these methods, but they **rely on good friction modelling and reasonably accurate dynamics**.

Bibliography

[1] Stanford Institute for Human-Centered Artificial Intelligence (HAI). "Artificial intelligence index report 2025," Accessed: Nov. 22, 2025. [Online]. Available: https://hai.stanford.edu/ai-index/2025-ai-index-report

[2] International Federation of Robotics. "World robotics 2025 report." Press release, Sept. 25, 2025, Accessed: Nov. 22, 2025. [Online]. Available: https://ifr.org/ifr-press-releases/news/global-robot-demand-in-factories-doubles-over-10-years

[3] International Federation of Robotics. "Collaborative robots – how robots work alongside humans." Bar chart illustration, Accessed: Nov. 22, 2025. [Online]. Available: https://ifr.org/ifr-press-releases/news/how-robots-work-alongside-humans

[4] P. Nadeau, M. Giamou, and J. Kelly, "Fast object inertial parameter identification for collaborative robots," in 2022 International Conference on Robotics and Automation (ICRA), 2022, pp. 3560–3566. DOI: 10.1109/ICRA46639.2022.9916213

[5] A. Kurdas, M. Hamad, J. Vorndamme, N. Mansfeld, S. Abdolshah, and S. Haddadin, "Online payload identification for tactile robots using the momentum observer," in 2022 International Conference on Robotics and Automation (ICRA), 2022, pp. 5953–5959. DOI: 10.1109/ICRA46639.2022.9811691

[6] S. K. Kommuri, S. Han, and S. Lee, "External torque estimation using higher order sliding-mode observer for robot manipulators," IEEE/ASME Transactions on Mechatronics, vol. 27, no. 1, pp. 513–523, 2022. DOI: 10.1109/TMECH.2021.3067443

[7] S. Zhang, M. Yuan, Z. Huo, J. Huang, and X. Zhang, "Accurate payload dynamics estimation and compensation of a robotic manipulator without external motion measuring sensors," in 2025 11th International Conference on Electrical Engineering, Control and Robotics (EECR), 2025, pp. 1–8. DOI: 10.1109/EECR64516.2025.11077346

[8] M. Liu et al., "A two-stage payload dynamic parameter identification method for interactive industrial robots with large components," IEEE Transactions on Automation Science and Engineering, vol. 22, pp. 13 871–13 883, 2025. DOI: 10.1109/TASE.2025.3557064

[9] T. Xu et al., "Identifying current dynamics of robot payload based on iterative weighting estimation," IEEE Transactions on Instrumentation and Measurement, vol. 74, pp. 1–14, 2025. DOI: 10.1109/TIM.2025.3554883

[10] T. Xu, J. Fan, Q. Fang, Y. Zhu, and J. Zhao, "An accurate identification method based on double weighting for inertial parameters of robot payloads," Robotica, vol. 40, pp. 1–17, 2022. DOI: 10.1017/S0263574722000960 [Online]. Available: https://doi.org/10.1017/S0263574722000960

[11] J. Duan, Z. Liu, Y. Bin, K. Cui, and Z. Dai, "Payload identification and gravity/inertial compensation for six-dimensional force/torque sensor with a fast and robust trajectory design approach," Sensors, vol. 22, no. 2, 2022, ISSN: 1424-8220. DOI: 10.3390/s22020439 [Online]. Available: https://www.mdpi.com/1424-8220/22/2/439

[12] X. Wei et al., "Composite disturbance filtering for interaction force estimation with online environmental stiffness exploration," IEEE/ASME Transactions on Mechatronics, vol. 30, no. 1, pp. xxx–xxx, 2025. DOI: 10.1109/TMECH.2024.3443310

[13] J. Swevers, W. Verdonck, and J. De Schutter, "Dynamic model identification for industrial robots," IEEE Control Systems Magazine, vol. 27, no. 5, pp. 58–71, 2007. DOI: 10.1109/MCS.2007.904659

[14] S. Long, X. Dang, S. Sun, Y. Wang, and M. Gui, "A novel sliding mode momentum observer for collaborative robot collision detection," Machines, vol. 10, no. 9, p. 818, 2022. DOI: 10.3390/machines10090818 [Online]. Available: https://www.mdpi.com/2075-1702/10/9/818

[15] Z. Lao, Y. Han, Y. Ma, and G. S. Chirikjian, "A learning-based approach for estimating inertial properties of unknown objects from encoder discrepancies," IEEE Robotics and Automation Letters, vol. 8, no. 9, pp. 5283–5290, 2023. DOI: 10.1109/LRA.2023.3293723

[16] M. Tang, Y. Yan, B. An, W. Wang, and Y. Zhang, "Dynamic parameter identification of collaborative robot based on wls-rwpso algorithm," Machines, vol. 11, no. 2, p. 316, 2023. DOI: 10.3390/machines11020316 [Online]. Available: https://www.mdpi.com/2075-1702/11/2/316

[17] J. Hu, Z. Chen, Y. Lin, Z. Chen, B. Yao, and X. Ma, "On the fully decoupled rigid-body dynamics identification of serial industrial robots," IEEE Transactions on Robotics, vol. 41, pp. 4588–4605, 2025. DOI: 10.1109/TRO.2025.3578229

List of Figures

List of Tables

List of source codes

A Appendix Kinematic and Dynamic Background of Robot Manipulation and Environment Interaction

The external wrench $\vec{F}_{\text{ext}}$ in (5) is a 6-dimensional vector expressed in the sensor/tool frame S,

$$\vec{F}_{\text{ext}} = \begin{bmatrix} \mathbf{f} \\ \boldsymbol{\tau} \end{bmatrix} \in \mathbb{R}^6, \tag{9}$$

with $\mathbf{f} \in \mathbb{R}^3$ the linear force and $\boldsymbol{\tau} \in \mathbb{R}^3$ the moment about the frame origin. For a rigid body with parameters ϕ_{eff} (mass, CoM and inertia) moving with linear and angular motion $(\mathbf{a}, \boldsymbol{\alpha}, \boldsymbol{\omega})$, the Newton–Euler equations (cf. (2)) give

$$\begin{bmatrix} \mathbf{f} \\ \boldsymbol{\tau} \end{bmatrix} = m \begin{bmatrix} \mathbf{I} & -[\mathbf{c}]^\times \\ [\mathbf{c}]^\times & \mathbf{J}_s \end{bmatrix} \begin{bmatrix} \mathbf{a} \\ \boldsymbol{\alpha} \end{bmatrix} + \begin{bmatrix} m[\boldsymbol{\omega}]^\times[\boldsymbol{\omega}]^\times \mathbf{c} \\ [\boldsymbol{\omega}]^\times \mathbf{J}_s \boldsymbol{\omega} \end{bmatrix}. \tag{10}$$

The translational part $\mathbf{f}$ can be written as

$$\mathbf{f} = m\mathbf{a} - m[\mathbf{c}]^\times \boldsymbol{\alpha} + m[\boldsymbol{\omega}]^\times[\boldsymbol{\omega}]^\times \mathbf{c}, \tag{11}$$

where the first term $m\mathbf{a}$ is the familiar inertial force, while $-m[\mathbf{c}]^\times \boldsymbol{\alpha}$ and $m[\boldsymbol{\omega}]^\times[\boldsymbol{\omega}]^\times \mathbf{c}$ collect the additional centripetal and Coriolis contributions induced by the angular motion $\boldsymbol{\omega}$ and the CoM offset $\mathbf{c}$. Similarly, the rotational part $\boldsymbol{\tau}$ can be written as

$$\boldsymbol{\tau} = m[\mathbf{c}]^\times \mathbf{a} + \mathbf{J}_s \boldsymbol{\alpha} + [\boldsymbol{\omega}]^\times \mathbf{J}_s \boldsymbol{\omega}, \tag{12}$$

where $\mathbf{J}_s \boldsymbol{\alpha}$ is the inertial moment due to angular acceleration, $m[\mathbf{c}]^\times \mathbf{a}$ is the torque induced by the translational acceleration of the offset CoM, and $[\boldsymbol{\omega}]^\times \mathbf{J}_s \boldsymbol{\omega}$ represents gyroscopic effects associated with the angular velocity $\boldsymbol{\omega}$.

In compact form, for a given motion $(\mathbf{a}, \boldsymbol{\alpha}, \boldsymbol{\omega})$ this can be written as

$$\vec{F}_{\text{ext}} = \vec{F}_{\text{dyn}}(\mathbf{a}, \boldsymbol{\alpha}, \boldsymbol{\omega}; \phi_{\text{eff}}) = Y(\mathbf{a}, \boldsymbol{\alpha}, \boldsymbol{\omega})\, \phi_{\text{eff}}, \tag{13}$$

where $Y(\cdot)$ is a 6×10 regressor matrix that is linear in ϕ_{eff} but nonlinear in the motion variables. Hence, $\vec{F}_{\text{ext}}$ is not simply $m\mathbf{a}$, nor can it be written as $\phi_{\text{eff}}\ddot{\mathbf{q}}$; the mapping from joint accelerations $\ddot{\mathbf{q}}$ to $\vec{F}_{\text{ext}}$ passes through the robot kinematics and the Newton–Euler relations.

Once the wrench at the flange is known, the corresponding joint torques are obtained via

$$\boldsymbol{\tau}_{\text{ext}} = {}^S J(\mathbf{q})^\top \vec{F}_{\text{ext}}, \tag{14}$$

where $^{S}J(\mathbf{q})$ is the Jacobian of the sensor/tool frame S. Combining the relations above yields the identification-friendly form

$$\boldsymbol{\tau}_{\text{ext}} = \mathbf{J}^{T}(\mathbf{q})\, Y(\mathbf{a}, \boldsymbol{\alpha}, \boldsymbol{\omega})\, \boldsymbol{\phi}_{\text{eff}}, \tag{15}$$

which makes explicit that $\boldsymbol{\tau}_{\text{ext}}$ is linear in $\boldsymbol{\phi}_{\text{eff}}$, but nonlinear in $\mathbf{q}, \dot{\mathbf{q}}, \ddot{\mathbf{q}}$ through the dependence on $\mathbf{a}, \boldsymbol{\alpha}, \boldsymbol{\omega}$.

B Appendix B